

Citation for published version:

Bouzekri Amina, Allaoui Tayeb, and Denai Mouloud, 'Intelligent Open Switch Fault Detection for Power Converter in Wind Energy System', *Applied Artificial Intelligence*, Vol. 30 (9): 886-898, February 2017.

DOI:

<https://doi.org/10.1080/08839514.2016.1277294>

Document Version:

This is the Accepted Manuscript version.

The version in the University of Hertfordshire Research Archive may differ from the final published version.

Copyright and Reuse:

© 2017 The Authors. Published by Taylor & Francis.

Content in the UH Research Archive is made available for personal research, educational, and non-commercial purposes only. Unless otherwise stated, all content is protected by copyright, and in the absence of an open license, permissions for further re-use should be sought from the publisher, the author, or other copyright holder.

Enquiries

If you believe this document infringes copyright, please contact the Research & Scholarly Communications Team at rsc@herts.ac.uk

Intelligent Open Switch Fault Detection for Power Converter in Wind Energy System

A. BOUZEKRI [†], T. ALLAOUI ^{*}, M. DENAI ^{**}

^{†*} Laboratory of Electrical and Computer Engineering (L2GEGI), Ibn Khaldun University, Tiaret, Algeria

bouzekriamina@hotmail.fr , allaoui_tb@yahoo.fr

^{**} School of Engineering and Technology, University of Hertfordshire, Hatfield, United Kingdom

Abstract

This paper proposes a simple and fast fuzzy logic-based open-switch fault detection method for rotor side converter in doubly-fed induction generator (DFIG) wind turbine system. In the proposed scheme, only the mean values of the three-phase rotor currents are used to identify the power switch in which the open circuit fault has occurred.

The wind energy conversion system model developed for the design and evaluation of the proposed fault detection technique includes a DFIG-based wind turbine with maximum power point tracking (MPPT) control strategy, a rotor side converter (RSC) to control the electromagnetic torque and stator reactive power and a grid side converter (GSC) to regulate the DC link voltage at the desired level. The simulation model was developed in Matlab/Simulink environment. The results show that the proposed fault detection scheme is able to rapidly and effectively identify open switch faults among other fault types in a time less than one period.

I. INTRODUCTION

Wind energy is rapidly developing as one of the most prominent renewable energy source in the world. By the end of 2020, it is expected that wind power generation will increase to 1.26 million of MW which will be sufficient to cover 12% of the world's electricity consumption [1]. Various wind turbine configurations using different generator topologies have been extensively studied, developed and built. There are two main types of wind turbines systems: the Fixed-Speed Wind Turbine (FSWT) and the Variable-Speed Wind Turbine (VSWT). The FSWT uses a multistage gearbox and a squirrel cage induction generator (SCIG) and is directly connected to the grid. The FSWT uses a multistage

gearbox and a Doubly-Fed Induction Generator (DFIG) and is connected to the grid via a power electronic converter. VSWT has become the most popular type of wind turbine system because it uses a power electronic converter which offers better control capability than the FSWT [2, 3].

Electrical energy providers strive to ensure that the electricity supplied across their broad range of customers meets a reasonable quality. Broadly, the term electric power quality refers to two aspects: (i) the provision of continuity of supply and essential service (ii) maintaining a stable, near sinusoidal supply voltage at rated magnitude and frequency. The first one relates to the reliability of energy distribution and the quality of the services provided to users whereas the second encompasses the disturbances related to the voltage supplied by the network such as overvoltage, voltage unbalance; voltage dips and interruptions, harmonics and power-frequency variations. The latter one characterizes the relationship between the user and the system operator.

In electrical networks, the voltage waveform must ideally have the sinusoidal waveform with a constant frequency and magnitude. However, in reality, the voltage waveform is never perfectly sinusoidal, the frequency and amplitude of the wave continuously fluctuate, and may sometimes deviate significantly from their reference values. These disturbances in the voltage waveform can compromise the normal operation of sensitive loads connected to the network. It is estimated that about 38% of the faults in industrial variable-speed ac drives are the result of failures of converter power devices [ref]. Faults in power converters can be broadly classified as short-circuit faults and open-circuit faults. Short-circuit faults represent the most serious class of fault which in most situations cause an over current that can be dealt with by standard protection devices. However, open-circuit failures, which may occur when, for some reason, the semiconductor device is disconnected, damaged or due to a malfunction in the gate control signal, do not trigger any protection device.

There has been an extensive research in the area of fault diagnosis and detection in converter power switches. In [reference] has presented a comparative literature review on the existing methods for IGBT diagnostics and protection, including open-circuit, short-circuit, and gate-misfiring faults. More than 20 methods for open-circuit fault and 10 methods for short-circuit fault diagnosis have been evaluated and compared in terms of effectiveness, resistivity, detection time, implantation effort and

tuning effort. Among the open-circuit fault methods, the wavelet, fuzzy, and neural network-based methods render additional intelligence for smart diagnosis which have a high results then all the others method. In [2], the development of a complete artificial-neural-network space- vector- modulation and diagnostic controller has been done for a four-switch three-phase inverter. In this paper, we will use a fuzzy logic based method to detect an open circuit fault for a rotor side converter in Doubly Fed Induction Generator (DFIG) wind energy system in order to avoid any disaster in the system and grid.

II. DFIG-BASED WIND POWER SYSTEM MODELLING AND CONTROL

The proposed DFIG-based wind turbine system is shown in Fig. 1. The DFIG has 3-phase supply in the stator and 3-phase supply in the rotor. The rotor is coupled via two powers converters: the rotor-side converter (RSC) and the grid-side converter (GSC). The RSC provides a decoupling between the active and reactive stator power control, P_s and Q_s according to the reference torque delivered by the maximum power point tracking control (MPPT). The GSC controls the power flow exchange with the grid via the rotor, by maintaining the DC bus at a constant voltage level.

1) Maximum power point tracking (MPPT)

Due to the intermittent and variable nature of wind power, it is desirable to determine the optimal generator speed which extracts the maximum power from the turbine. MPPT allows the variable-speed wind turbine to operate at an optimal speed depending on the wind speed and capture the maximum power from the available wind energy. Several MPPT control strategies have been proposed in the literature [13, 14]. The MPPT method used in this paper is termed Tip Speed Rotor (TSR) control [15]. This method regulates the rational speed of the generator in order to maintain the TSR to an optimal value at which the power extracted is maximum. It requires both the wind speed and the turbine speed to be measured or estimated in addition to the knowledge of the optimal TSR of the turbine in order to be able extract maximum possible power. Fig. 2 shows the block diagram of a MPPT control with TSR control.

Where R is the radius of the wind turbine, λ_{opt} is the optimal TSR of the turbine and G is the inverted gain of the reducer.

The transfer function relating the mechanical speed and the electromagnetic torque is:

$$G_{MPPT}(s) = \frac{1}{Js + F} \quad Eq. (1)$$

Where J and F represent the inertia and friction coefficient of the overall system respectively. The closed-loop transfer function of the speed control loop including the proportional integral (PI) controller with gains $K_{p\Omega}$ and $K_{i\Omega}$ is obtained as:

$$H_{MPPT}(s) = \frac{K_{p\Omega} \left(s + \frac{K_{i\Omega}}{K_{p\Omega}} \right) / J}{s^2 + \left(\frac{F + K_{p\Omega}}{J} \right) s + \frac{K_{i\Omega}}{J}} \quad Eq. (2)$$

2) Rotor-Side Converter Control

The DFIG is connected directly to the network through the stator, and controlled by its rotor through an ideal AC/AC direct converter. Vector control based on direct stator flux orientation is used to control power exchange between the stator and the network [5, 2, 16]. Fig. 3 shows a schematic diagram of the RSC control.

The active and reactive stator powers and the electromagnetic torque of the DFIG in the Park frame are written as follows [4, 5]:

$$P_s = -V_{sq} \frac{M_{sr}}{L_s} I_{rq} \quad (3)$$

$$Q_s = V_{sq} \frac{\varphi_{sd}}{L_s} - V_{sq} \frac{M_{sr}}{L_s} I_{rd} \quad (4)$$

$$T = -p \frac{M_{sr}}{L_s} \varphi_{sd} I_{rq} \quad (5)$$

Where M_{sr} , L_s and p are respectively the main inductance and the inductance of the stator and number of pair poles.

Equations (3) and (4) show that the stator powers can be controlled via the rotor currents. There transfer function is shown as:

$$G_{I_{rd,q}}(s) = \frac{1}{\sigma L_r s + R_r} \quad (6)$$

The system performance can be enhanced if the rotor currents I_{rd} and I_{rq} are decoupled by adding e_{rq} term to the output of the d-axis current controller, and e_{rd} and e_φ to the output of the q-axis current controller [6], [22].

Where;

$$\begin{cases} e_{rd} = -\sigma L_r \omega_r L_{rq} \\ e_{rq} = \sigma L_r \omega_r L_{rd} \\ e_\varphi = \omega_r \frac{M_{sr}}{L_s} \varphi_{sd} \end{cases} \quad (7)$$

3) Grid-Side Converter Control

The GSC is connected between the grid via RL filter and the DC-link. The role of this converter is to maintain the DC-link voltage as the constant value [2, 16]. The control of this voltage is achieved through the control of the rectifier currents as shown in the Fig. 4.

The DC-voltage signal V_{dc} is compared to its reference signal V_{dc}^* and the error signal from inputs to the PI regulator which generates the reference amplitude current I_{max} . This amplitude multiples with a three phases sinusoidal functions have a same input voltage frequency and compared with measurements grid currents to generate the switching pulse for the converter through the PWM block.

4) Simulation of the wind power system model and controllers

The overall system model is simulation using MATLAB/Simulink. In the following simulations, the wind power system is assumed to operate in the zone of optimal functioning. The DFIG is rated at 7.5 kW and its parameters are listed in Table 1.

Extensive simulations were performed to evaluate the performance of the vector-controlled DFIG. The simulations results are presented in the Fig. 7. Fig. 7a shows the wind speed profile applied to the wind turbine blades with an average value of 7 m/s, which corresponds to the speed of DFIG under MPPT control as shown Fig. 7b. Fig. 7e and 7f show the active and reactive stator powers (Q_s, P_s) delivered in the grid.

III. THE PROPOSED FAULT DETECTION METHOD

1) Open-switch fault rotor side converter

The shape of the currents pattern in a healthy condition is shown in Fig.7. A fault was created in one switch among the six of rotor side converter. When the fault occurred, the quadrature and the direct rotor side currents increase considerably as shown Fig. 7a. Fig.7b shows the variation occurring in the DC link current with an enlarged view.Fig.7c shows the alternative rotor current and the three-phase stator currents delivered in the grid. These effects of the fault on the system may cause unscheduled shutdown of the devise using or the deterioration of some equipment.

Fig. 8 represents the average values of three-phase rotor side converter currents. In the healthy condition the average values of the currents are almost zero (between $\pm 2 \cdot 10^{-4}$). However, under fault conditions, they assume other values. Table 2 shows the mean values of the three-phase rotor currents for the six switch open fault.

2) Fuzzy logic based open switch fault detection

The mean values of a three phase currents change from threshold value when the fault occurred. Therefore, the different cases given in Table 2 permit the detection of any open switch fault in the rotor side converter and identify it among the six switches. Fig. 9 shows the fuzzy logic method of open switch fault detection (IGBT with Anti-Parallel Diode), where the three-phase currents rotor side converter had been measured to calculate their average values (I_{ra_avg} , I_{rb_avg} and I_{rc_avg}) which are using in fuzzy logic method detection block. This principle of the method is illustrated by the flow chart of Fig. 10.

The fuzzy sets are designated by the labels: S (negative), Z (zero) and P (positive).Table2 shows the rules of detection fault. The membership functions for the input variables which present the average values of I_{ra} , I_{rb} , I_{rc} and the output variable surface which is the number switch fault are shown in Fig. 11. Sugeno-type fuzzy inference system was used and defuzzification was based on the centre of gravity method.

3) Simulation results

Figs.12 shows an open switch fault detection when the fault is in the first switch IGBT1 (fig12a), in the second switch IGBT2 (fig12b) and in the third switch IGBT3 (fig12c), where we have numbered

the switches as follow: give 1 , 2 and 3 for the upper switches starting by the rotor side switch and 4, 5 and 6 for the bottom switches.

So, when the fault was in the first switch the output of fuzzy logic block must a constant value equal 1, and it's same for the other switch. For the first [figure12a](#), the time of detection equals 0.015 s (means $\frac{2}{3}$ of one period); in the second [fig12b](#) equals 0.01 s (means $\frac{1}{3}$ of one period) and in the last one [fig12c](#) 0.005 s (means $\frac{1}{4}$ of one period). As we see, this method is efficiency detect and identify the fault switch with a very short detection time especially in the third one.

IV. CONCLUSION

This paper divided in two sections, the first one presented a global system of doubly fed induction generator wind turbine system and their controls strategy, which are the maximum power point tacking control (MPPT), the rotor side converter control (RSC) which controlling the electromagnetic torque and stator reactive power and the control of grid side converter (GSC) by controlling the DC link voltage.

The second section, presented an open switch fault detection method based on fuzzy logic inference. The fault in switch is detected, when the signal of three-phase average values of rotor currents are accordingly the preset detection threshold. The simulation results were showed the affectivity of this method and its fast detection which is less than one period in addition of its simplicity.

V. REFERENCES

VI. TABLES

Table 1 System parameters.

Rated power	7.5 Kw	R_s	0.455 Ω
Stator voltage	220 V	R_r	0.62 Ω
Stator/rotor turns ratio	1	L_s	0.084 H
Turbine power	10 Kw	L_r	0.081 H
Radius pale	3 m	M_{sr}	0.078 H
Reducer gain G	5.4	C filter	2 mF
Lumped inertia constant	0.3125	L_f filter	0.014 H
Number of pole pairs	2	R_f filter	0.3 Ω
DC Link voltage	800 V		
Switching frequency F_s	10 kHz		

Table 2 Average values of three-phase currents under different open switch fault.

I_{ra_avg}	I_{rb_avg}	I_{rc_avg}	Combination	Switch fault
1	-1	-1	1	S1 fault
-1	-1	1	2	S2 fault
-1	1	-1	3	S3 fault
-1	1	1	4	S4 fault
1	1	-1	5	S5 fault
1	-1	1	6	S6 fault
0	0	0	0	No fault

Table 3 Rules of the fuzzy logic-based open switch fault detection.

I_{ra_avg}	I_{rb_avg}	I_{rc_avg}	Number switch fault	Switch fault
P	S	S	1	S1 fault
S	S	P	2	S2 fault
S	P	S	3	S3 fault
S	P	P	4	S4 fault
P	P	S	5	S5 fault
P	S	P	6	S6 fault
Z	Z	Z	0	No fault

VII. FIGURES

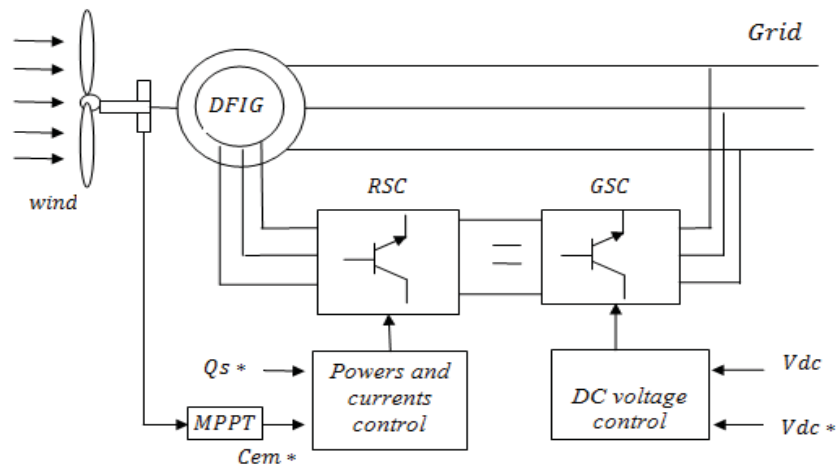


Fig.1 Block diagram of the wind power system based in DFIG.

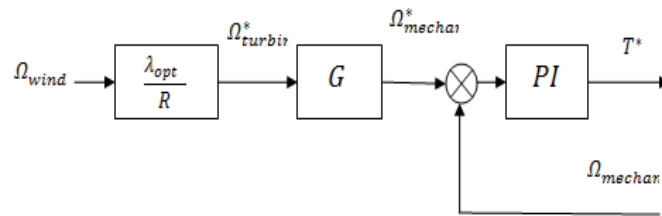


Fig.2 MPPT control.

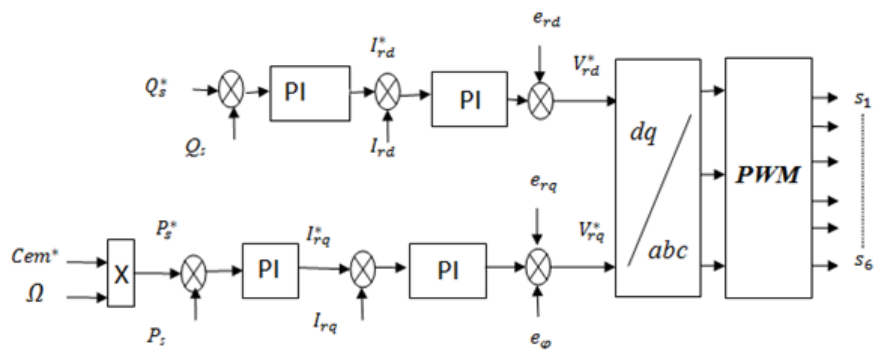


Fig. 3 Block diagram for the RSC control.

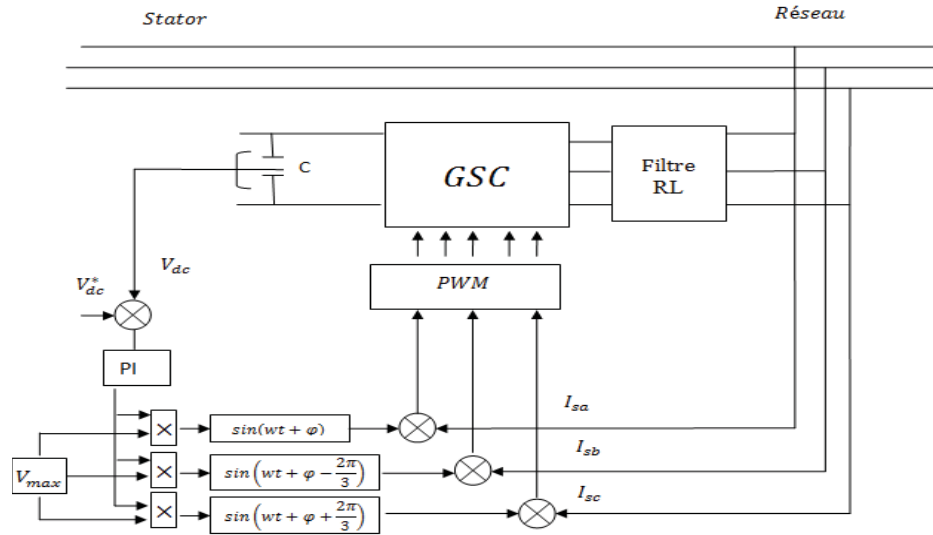


Figure 4 Block diagram for the GSC control.

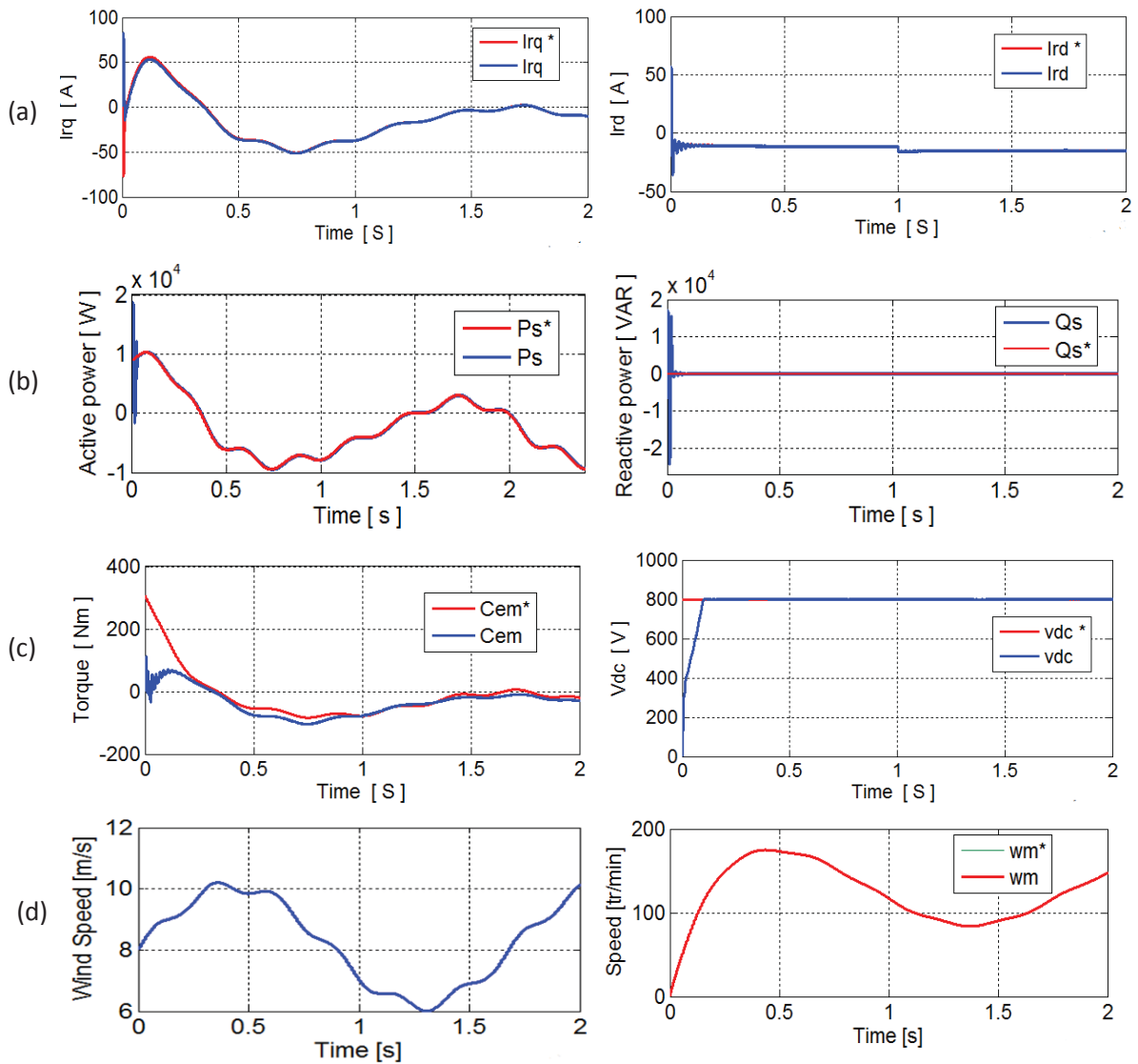
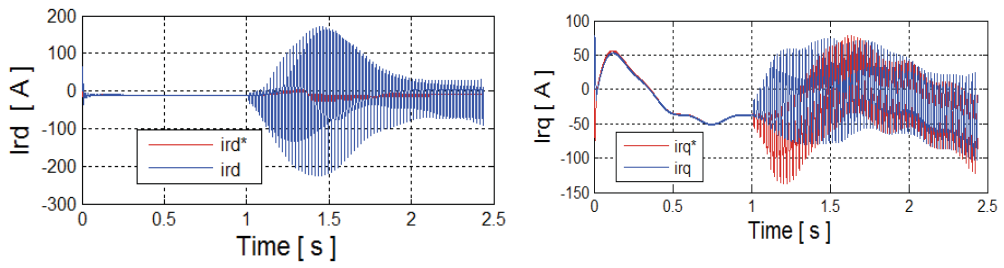
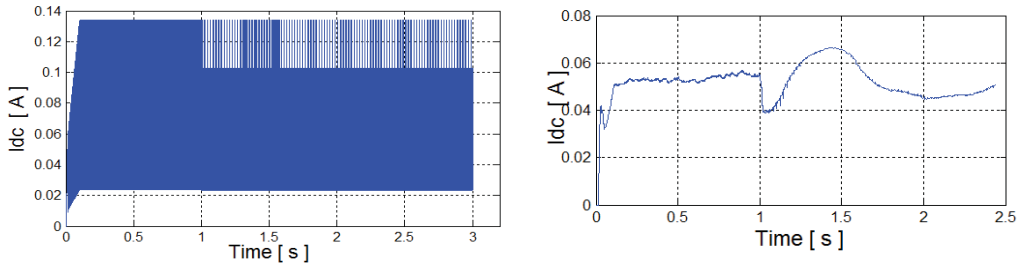


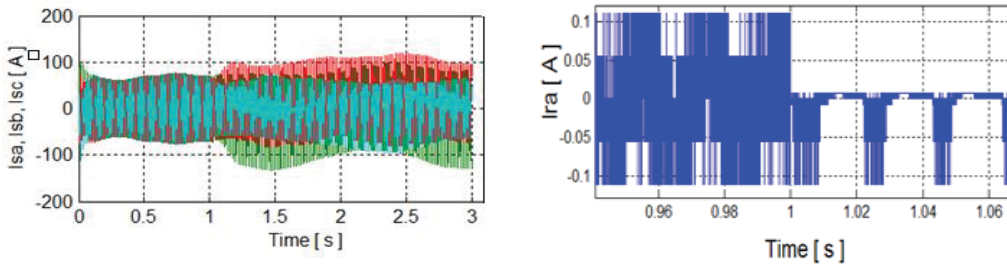
Fig. 5 (a) I_{rq} current, I_{rd} Current ; (b) active and reactive powers P_s , Q_s ; (c) Torque C_{em} , V_{dc} voltage; (d) Wind speed and Speed of DFIG with MPPT,



(a)



(b)



(c)

Fig.6 Open-switch effects on the currents (a) direct and quadrature rotor currents, (b) continuous current, (c) three-phase stator currents and rotor current phase.

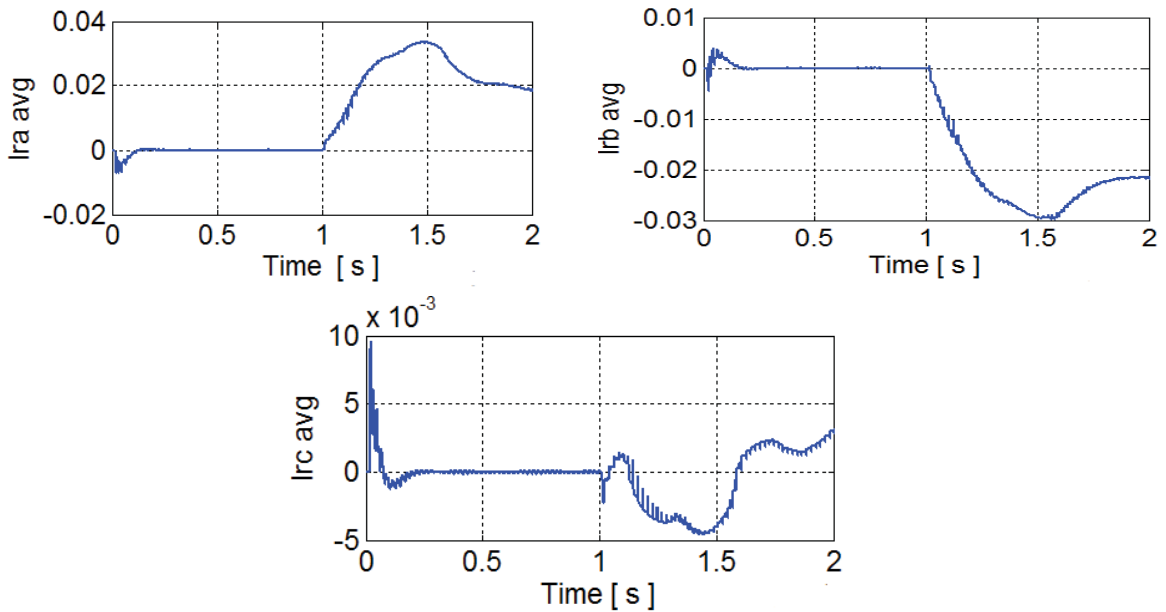


Fig.7 Three-phase rotor side converter currents mean values.

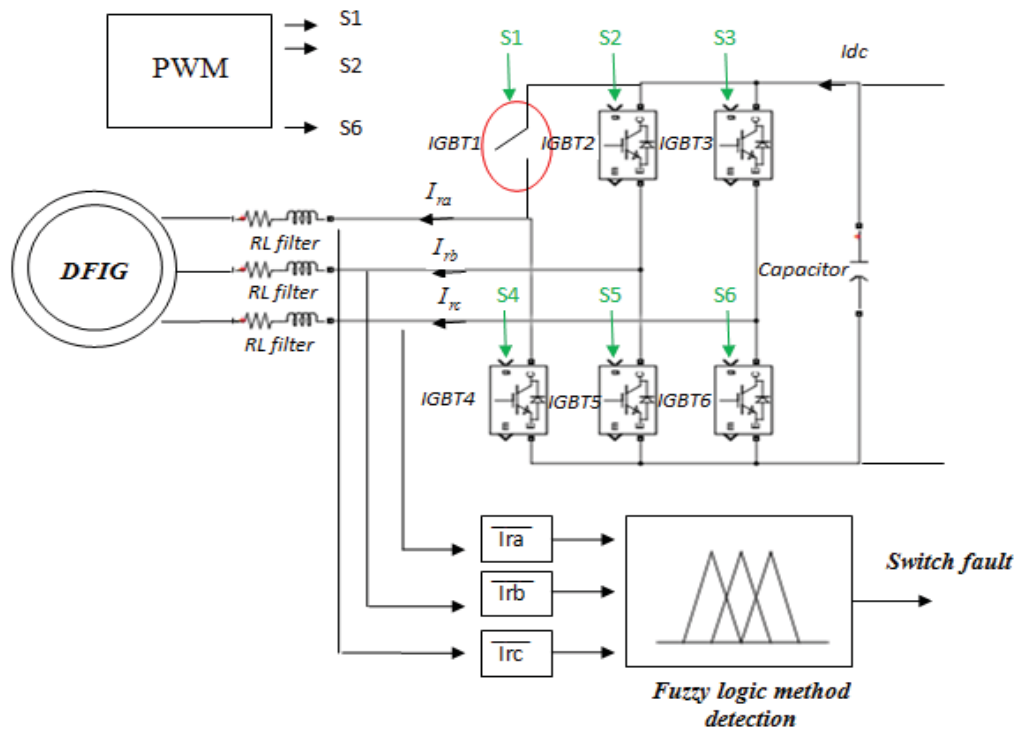


Fig.8 Block diagram of fuzzy logic method of open switch fault detection.

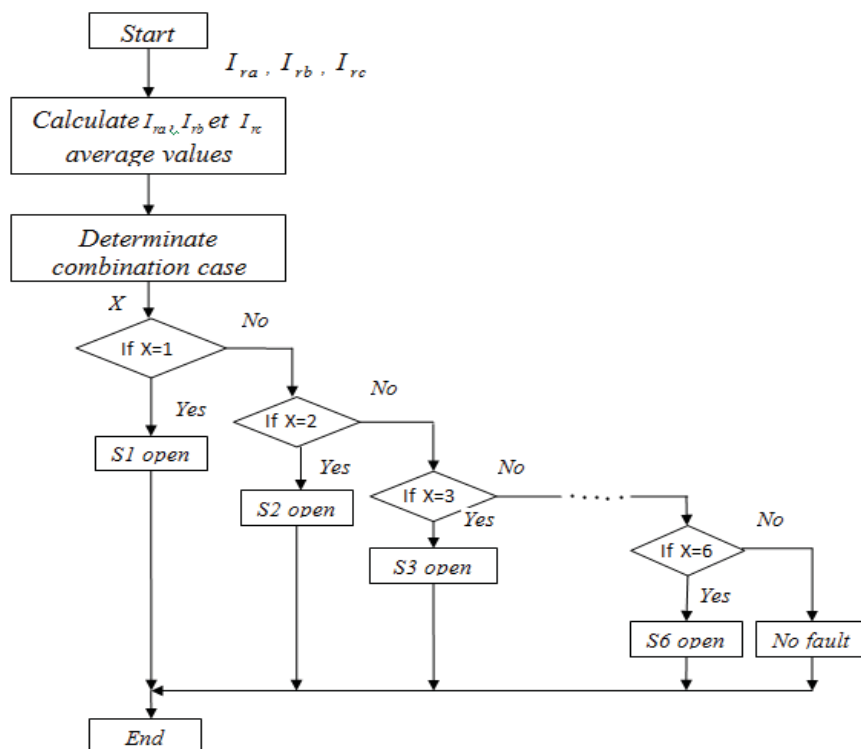


Fig.9 Flowchart of the fuzzy logic-based open switch fault detection method.

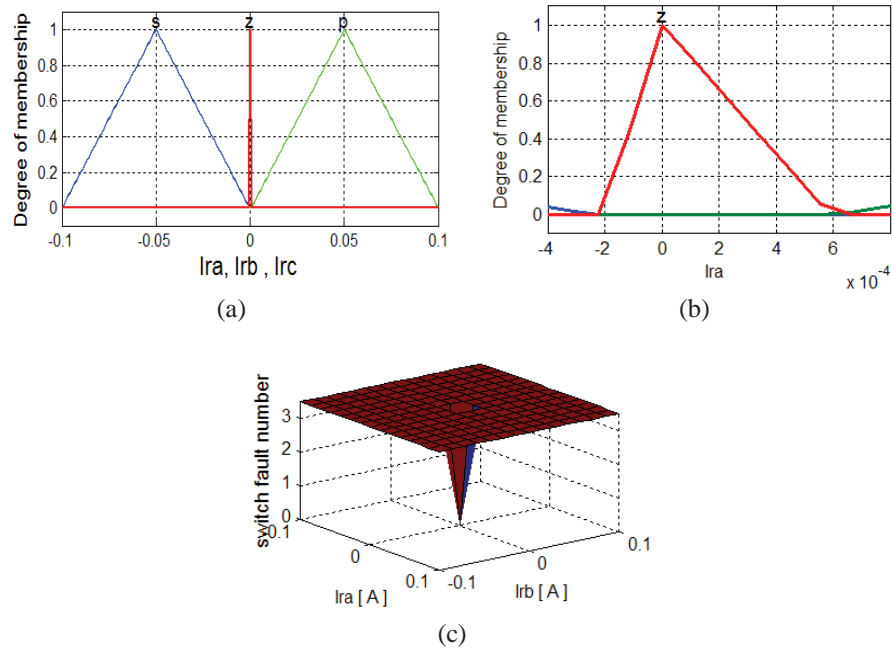


Fig.10 Membership functions of input fuzzy logic block and surface.

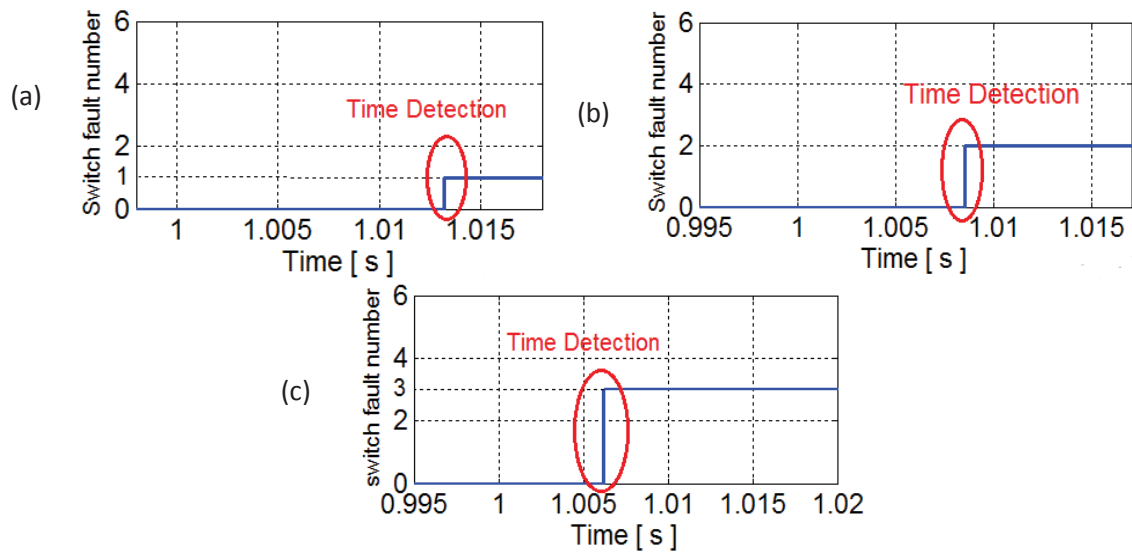


Figure 11 open switch fault detection (a) IGBT1, (b) IGBT2 and (c) IGBT3